J. Membrane Biol. 154, 23–33 (1996)

The Journal of
Membrane
Biology

© Springer-Verlag New York Inc. 1996

Heterogeneity of Volume-sensitive Chloride Channels in Basolateral Membranes of A6 Epithelial Cells in Culture

U. Banderali, J. Ehrenfeld
CEA and CNRS (URA 1855), Laboratoire Jean Maetz. B.P. 68, La Darse. 06230, Villefranche-sur-mer, France

Received: 17 April 1996/Revised: 26 June 1996

Abstract. A new technique allowing single-channel patch-clamp recordings from basolateral membranes of A6 renal epithelial cells in culture was developed. Using this technique we studied the chloride channels activated in these basolateral membranes during hypo-osmotic stress. Four different types of channel were identified and classified according to their current/voltage (*I/V*) relationships as observed in the on-cell configuration of the patch-clamp technique. Three of these channels had linear *I/V* relationships with unitary conductances of 12, 30 and 42 pS. The fourth type had an outwardly rectifying *I/V* curve with inward and outward conductances of 16 and 57 pS respectively. The kinetic properties of each class of channel were studied and kinetic models developed for two of them: the 42 pS channel and the outward rectifier. These models permitted the study of the evolution of the kinetic parameters during hypo-osmotic shock and revealed two different kinetic schemes of channel activation. The results of experiments made on the basolateral membranes were also compared with those of a set of analogous patch-clamp experiments carried out on isolated A6 cells. In these latter, the frequency of successful observations of active channels in a patch was 13%, whereas it was 31% for basolateral membranes. Also, of the four types of channel observed in basolateral membranes, two were never found in isolated cells, only the 12 pS channel and the outward rectifier were present in these isolated cells.

Key words: Chloride channels — Basolateral membranes — Volume regulation — Hypo-osmotic shock — Patch clamp — Epithelial cells — Isolated cells

Correspondence to: U. Banderali

Introduction

The A6 cultured cell line, derived from the distal region of *Xenopus laevis* kidney, is a model of a tight epithelium. A monolayer of A6 cells grown on a permeable support forms an epithelium performing transepithelial transport of Na^+ and Cl^- ions under hormonal regulation. A6 cells have also been reported to regulate their volume after swelling (RVD) following either a hypo-osmotic challenge or an alteration in transepithelial transport rate [5, 11, 26]. The mechanism underlying the cellular response to swelling is the extrusion of cytoplasmic osmolytes, principally K^+ and Cl^- ions, coupled with water efflux. In previous studies on the A6 cell line, it was shown that the basolateral membranes play a key role in RVD. In fact, the cellular response to swelling involves the stimulation of separate conductance pathways for potassium and chloride ions located in the basolateral membranes [5, 6, 11]. Most of the data on the behavior of A6 cells during RVD were obtained from macroscopic observation of cellular monolayers or entire cells, using techniques such as short-circuit current, isotope fluxes, spectrofluorimetry and whole-cell patch clamp [5, 11, 12]. Very little information about the characteristics of the volume-sensitive ion channels of A6 cells is as yet available largely because of the difficulty of access of patch-clamp pipettes to the basolateral side of polarized cell monolayers grown on filters. Direct observations of volume-sensitive ion channels have been made on other epithelial cells [3, 21, 22, 31, 35]. In a recent work on isolated A6 cells in subconfluent cultures, Nilius et al. [23] reported data on the activation of a potassium channel and a chloride channel by a hypo-osmotic shock at the single-channel level. However, a major problem arises when working on subconfluent cell cultures because full polarization and development of membrane transport mechanisms generally only occur after cell cul-

tures have grown to confluence. In the present work, we use a new technique, derived from that developed by Aceves and Erlij [1] with frog skin epithelium, allowing an entire cell monolayer to be detached from the culture filter and turned upside down to expose basolateral membranes to patch-clamp pipettes. With this technique, we studied the volume-sensitive basolateral chloride channels at the single-channel level. We showed that hypo-osmotic stress can activate at least four different types of chloride channel. These channels are classified according to their unitary conductances and kinetic properties, as observed from on-cell recordings. We also compared the results obtained on basolateral membranes with those of analogous experiments made on isolated A6 cells and we showed that both the frequency of observation of chloride channels and the number of different types of channel observed were higher in basolateral membranes than in isolated cells.

Materials and Methods

Cell Culture

The A6 cell line was a gift of Dr. Rossier (Lausanne, Switzerland). It was originally obtained from the American Tissue Type Collection and subsequently cloned (clone A6-2F3) by limiting dilution [34]. Cells were grown between passages 88 to 98 at 28°C in a humidified atmosphere of 5% CO_2 in air. The amphibian cell medium (AM) [15] with the addition of 100 g/l fetal calf serum (IBF, France) and antibiotics, was changed three times weekly for cell nourishment.

Patch-Clamp Technique

For patch-clamp experiments [14], the cells were seeded onto porous membranes in culture wells (Transwell-clear, 24 mm diameter, 0.4 μm pores, Costar, Cambridge, MA) at a density of 2×10^6 cells per well. Cell monolayers were then fed with serum-free amphibian medium supplemented with 20 g/l ultroser-G (Gibco-IBF, France) for 5–10 days. The patch electrodes were obtained from capillary glass micropipettes (Vitrex, Denmark) by a double pulling on a vertical puller (David Kopf, Tujunga, CA). The electrode resistance was 4 to 6 MΩ. The patch-clamp amplifier was a Biologic RK 300 (Claix, France) and the signal was recorded on magnetic tape with a betamax video recorder (Sony), after conversion to a video signal by a Biologic PCM converter (Claix, France). The signal was then analyzed using a Compaq ProLinea 4/50 microcomputer with Cambridge Electronic Design (Cambridge, U.K.) software and A/D interface. Single channel signals were filtered at 10 KHz and digitized at 20 KHz. The extracellular solution used during the experiments was a Ringer solution containing (mmol/l): NaCl 83, Na_2SO_4 12, Glucose 11, HEPES 5, Na_2HPO_4 3.2, KCl 2.5, $MgSO_4$ 2, $CaCl_2$ 2, KH_2PO_4 1.2, with a pH of 7.4. The hypo-osmotic solution was obtained by diluting the Ringer solution with 1/3 volume of water. The patch-clamp pipette solution contained (mmol/l): Choline-Cl 145, $CaCl_2$ 3, HEPES 5, with a pH adjusted to 7.3 with NaOH.

For experiments on isolated cells, the cells were prepared as described elsewhere [5]. Results are given as means ± SE. The voltages given in the graphs (*V*p) and in the text are the opposite of the actual pipette holding potential therefore, positive values of *V*p correspond to depolarizing voltages and negative values of *V*p correspond to hyperpolarizing voltages applied to the channel.

Access to Basolateral Membranes

A well containing a confluent monolayer of A6 cells was transferred to a petri dish filled with ≈1.5 ml of Ringer solution containing 1 g/l collagenase (Worthington, NJ) and 1 g/l albumin (Sigma) which thus bathed the basal side. The petri dish was kept in an incubator at 28°C for 15 to 30 min. The well was then removed from the petri dish and transferred to a Plexiglas Ussing-type chamber containing ≈13 ml collagenase-free Ringer solution in contact with the basal side. The lower (basal) compartment of this Ussing-type chamber communicated with an upright external tube (3 mm inner diameter) which after fixation of the well was filled with Ringer solution to establish a hydrostatic pressure difference of about 180 mm H_2O between the basal and apical compartments. Application of hydrostatic pressure for about 10 min resulted in the full detachment of the cell monolayer from the culture filter, except along its perimeter. The separation of the epithelium from the filter was clearly visible since the hydrostatic pressure arched the cell monolayer upwards, while the filter remained flat. Once this had taken place, the hydrostatic pressure was released, the well removed from the chamber and the solution in the apical compartment emptied out. The filter was then cut out of the well and transferred upside down onto a glass coverslip previously coated with RTV-2 elastomer (Rhodorsil RTV-2, Rhône-Poulenc, France). Thus the apical side of the epithelium was in contact with the elastomer. At this point two fine forceps were used to removed the filter while maintaining the epithelium on the slip with gentle pressure. The epithelium, its basolateral membrane exposed, was then fixed with an elastomer ring, leaving a small surface of the monolayer (20 mm^2) uncovered. Finally, a Plexiglas perfusion chamber was placed on top and the whole system mounted on the stage of an inverted microscope.

Computer Simulations

Kinetic models were developed by means of self-made simulation computer programs. The rate constants of the transitions between the different states of the channel ($k_{i \to j}$) were the adjustable parameters of a best-fit iterative procedure. The values of the rate constants were random numbers ranging initially between 0 and 500 sec^{-1} and were changed one at a time during each iteration. These random values were introduced in the equations, derived from the chosen kinetic model describing the open and closed dwell-time distributions and the open and closed probabilities. The results of these equations were then compared with the experimental data and the goodness of fit was evaluated from the χ^2 value. When a set of values for the rate constants in an iteration diminished the χ^2 value, it was stored as a set of final variables. The number of iterations in a program run was fixed at a value which was three times the number of iterations having led to the last decrease in the χ^2 value. At each χ^2 improvement, the best fitting rate constants were compared with the upper limit of the random numbers variation range (initially 500 sec^{-1}) and if their value was higher than 90% of the limit, this was automatically doubled.

Results

This study concerned the volume-sensitive chloride channels located in the basolateral membranes of A6

epithelial cells in culture. A cell monolayer was submitted to a hypo-osmotic shock while single-channel activity of the basolateral membranes was recorded with the technique described above, using pipettes filled with the choline-Cl solution. Under iso-osmotic conditions active chloride channels were observed in 8 out of 81 successful patches (i.e., 10% of patches). The hypo-osmotic challenge either increased the activity of an already functioning channel or stimulated a previously quiescent one within 5 min. Under these conditions, we recorded chloride channel activity in 25 of the 81 patches (i.e., 31%). In both cases, the various recordings showed a heterogeneous population of volume-sensitive chloride channels. Since inside-out recordings were not possible for all of the different types of channel observed due to rapid rundown of activity, we classified them according to their unitary conductance and to the rectifying properties of the *I/V* curves as observed in on-cell recordings. The channels were grouped in four classes: a small conductance channel of 12 pS, two intermediate conductance channels (30 and 42 pS) and an outward rectifying channel characterized by two unitary conductances of 16 and 57 pS for inward and outward currents respectively.

These results were compared with those obtained in a series of analogous patch-clamp experiments performed on isolated A6 cells. In these latter experiments, we observed single chloride channel activity in 4 out of 99 patches under iso-osmotic conditions (i.e., 4%) and in 13 patches under hypo-osmotic conditions (i.e., 13%). Only two different types of chloride channel were found in these experiments: the small conductance channel and the outward rectifier.

In the following sections we will describe the characteristics of each type of channel.

Small Conductance Channel (12 pS)

The small conductance channel was the most frequently found both in basolateral membranes ($n = 7$) and in isolated cells ($n = 5$).

This channel had a linear *I/V* relationship when recorded in the on-cell configuration (Fig. 1). The average single-channel conductance calculated from 12 observations was 12.4 ± 3.5 pS. In four patches the channel was active in iso-osmotic conditions and its activity increased after hypo-osmotic shock, as shown in Fig. 2*A*. However, the level of activity of this channel under iso-osmotic conditions was very low and its open probability (P_o) had a value close to zero. In all the other cases the activity started after the extracellular solution had been changed to the hypo-osmotic one. Under hypo-osmotic conditions, the open probability became 0.18 ± 0.06. The average delay between hypo-osmotic shock and stimulation of channel activity was 2.6 ± 0.5 min.

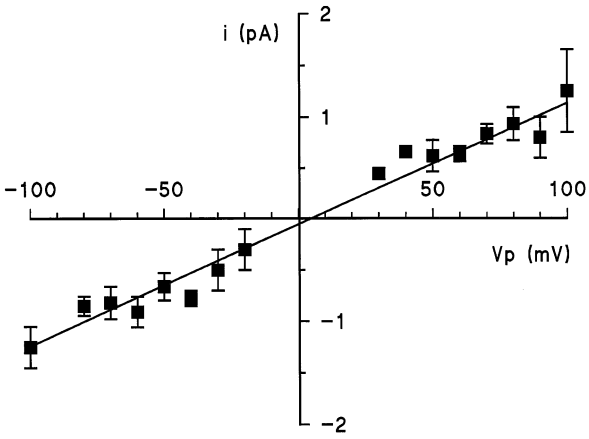

Fig. 1. Current/voltage relationship for the 12 pS channel. Average *I/V* curve obtained from the pooled recordings of the channel in basolateral membranes and in isolated cells ($n = 12$).

Figure 2 also shows examples of the distributions of open-time intervals (Fig. 2*B*) and closed-time intervals (Fig. 2*C*) from a recording of the channel during hypo-osmotic challenge. Due to the low activity of the channel when the cells were in the iso-osmotic solution, we were not able to obtain such distributions in control conditions. Both distributions could be fitted with single exponential functions, indicating that the channel had at least one open and one closed state. The average time constants were $\tau_O = 16.3 \pm 5.9$ msec for open time intervals and $\tau_C = 109.0 \pm 20.5$ msec for closed time intervals ($n = 5$) and did not change with voltage.

First Intermediate Conductance Channel (30 pS)

A channel characterized by a linear on-cell *I/V* relationship appeared in 4 of the 81 patches on the basolateral membranes (Fig. 3*A* and *B*), whereas it was never seen in isolated cells. Its average unitary conductance was 29.8 ± 2.4 pS. In only one case was the channel active in the iso-osmotic solution although with a value of P_o close to zero. Bathing the cells in hypo-osmotic solution activated this channel with delays ranging between 1.5 and 4 min, with a mean value of 2.8 ± 0.7 min. After activation P_o had a value of 0.27 ± 0.06. The distributions of open- and closed-time intervals were obtained from the recordings in the hypo-osmotic solution (Fig. 3*C* and *D*). A single exponential function was found to fit the distribution of closed-time intervals (Fig. 3*D*) giving an average time constant τ_C of 10.3 ± 3.9 msec, whereas the sum of two exponentials was necessary to fit the open interval distribution (Fig. 3*C*). We show the two exponential components fitting the distribution in the log-log plot [27] in the inset of Fig. 3*C* (broken lines). The mean

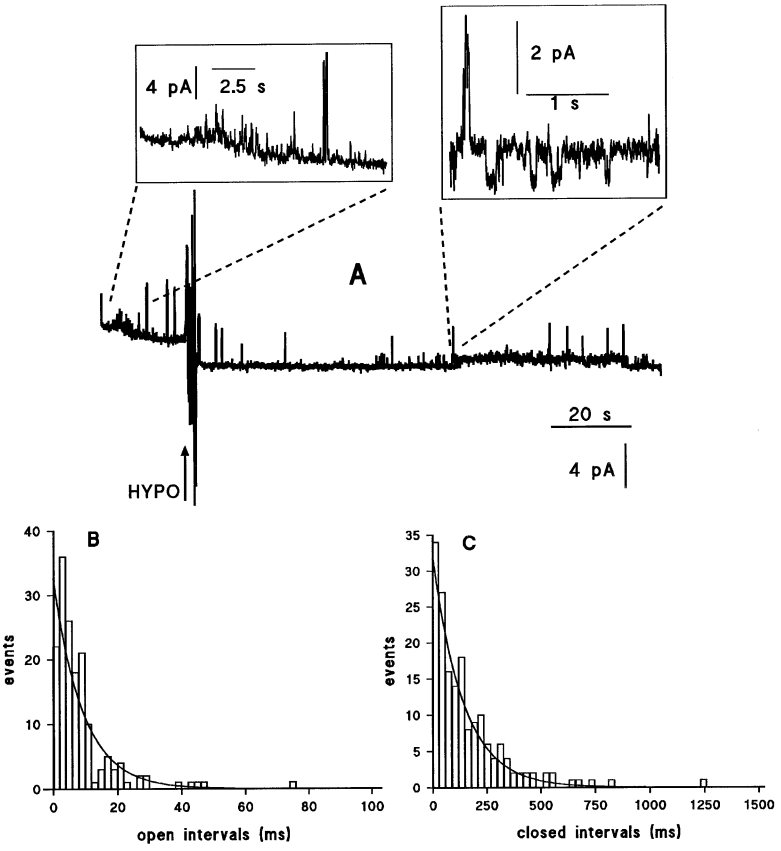

Fig. 2. Characterization of the 12 pS channel. (*A*) Activation of the small conductance channel by hypo-osmotic shock (arrow), recorded in the basolateral membrane of an A6 cell. The insets show details of the channel activity before and after the osmotic shock. A second channel with a higher unitary conductance was also present but its activity was not altered by hypo-osmotic shock. The recording was made with a holding potential of +50 mV. (*B*) Experimental distribution of the open dwell times (open bars) and best-fitting single exponential function (continuous line). (*C*) Experimental distribution of closed dwell times (open bars) and theoretical single exponential curve (continuous line). Both distributions were obtained in hypo-osmotic conditions analyzing 173 events.

values of the time constants of the exponential functions were: $\tau_{O1} = 19.4 \pm 2.3$ msec and $\tau_{O2} = 98.5 \pm 17.2$ msec. These results indicate that this channel has at least two open and one closed state. The time constants of both distributions were independent of voltage.

Second Intermediate Conductance Channel (42 pS)

A second intermediate conductance channel appeared exclusively in patches on the basolateral membranes. The *I/V* relationship of this channel in the on-cell recordings (Fig. 4*A* and *B*) was linear, with a unitary slope conductance of 42.1 ± 8.3 pS ($n = 6$). In two cases, the channel was active in the iso-osmotic solution with an open probability value of 0.36 ± 0.08 and hypo-osmotic shock increased P_o to a value of 0.53 ± 0.09. In the other cases the hypo-osmotic shock activated a quiescent channel. The delay between osmotic shock and channel response ranged between 1 and 5 min, with an average value of 2.7 ± 1.0 min. The distributions of open- and closed-time intervals were analyzed under both iso-osmotic and hypo-osmotic conditions. A simple exponential was found to fit the open-times distribution whereas a double exponential function gave the best fit for the closed-times histogram (Fig. 4*C* and *D*), indicating at least one possible open state and two possible closed states for the channel. The hypo-osmotic stress provoked an increase of the duration of the open dwell-times. In Fig. 4*C*, the histograms of open dwell-times in control conditions (solid bars) and after hypo-osmotic shock (open bars) are shown together with the exponential curves fitting the experimental data (continuous lines). The time constant τ_O of the exponential function in iso-osmotic conditions had a value of 56.8 ± 9.8 msec which increased to a value of 146.7 ± 22.8 msec during hypo-osmotic stress. The time constants of the exponentials fitting the closed intervals were $\tau_{C1} = 130.7 \pm 24.0$ msec and $\tau_{C2} = 5.6 \pm 1.4$ msec in iso-osmotic control conditions and became $\tau_{C1} = 68.8 \pm 6.0$ msec and $\tau_{C2} = 7.2 \pm 1.6$ msec in the hypo-osmotic solution. Figure 4*D* shows the histogram of closed dwell-times together with the double exponential curve under hypo-osmotic conditions and in the inset the log-log plot with the two exponential components (broken lines) is given. Based on these observations, we made a computer simulation of the activity of the channel starting from a kinetic model characterized by one open and two closed states: $C_1 \rightleftarrows C_2 \rightleftarrows O$. Table 1 summarizes the values of the rate constants $k_{i \to j}$ relative to the transitions between the different states under iso-osmotic and hypo-osmotic conditions and also the values of the probabilities of occupation of each of the states (P_{state}) as calculated from the model. Under iso-osmotic conditions, the channel

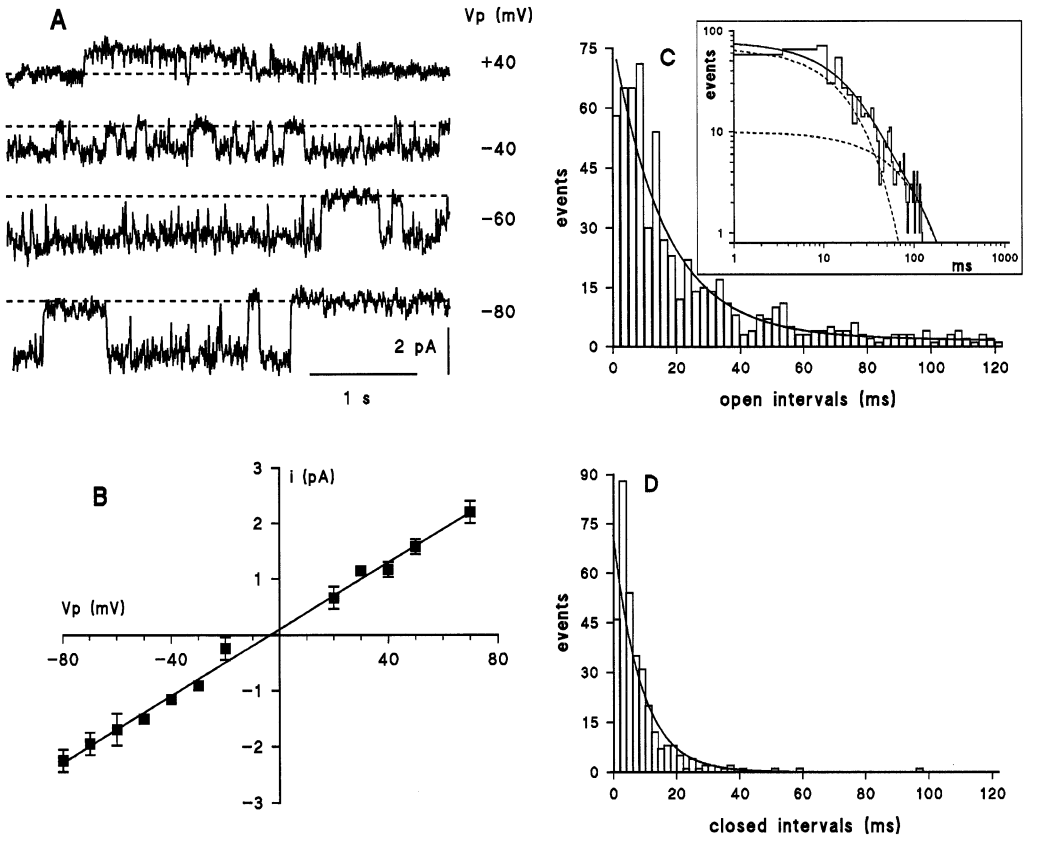

Fig. 3. Characterization of the 30 pS channel. (*A*) Recordings of channel activity at four different holding voltages. The broken lines indicate the closed-state current levels. (*B*) Current/voltage relationship of the channel averaging the data from four independent recordings. Experimental data were fitted by linear regression (continuous line). (*C*) Experimental open dwell-time distribution (open bars) and best-fitting double exponential function (continuous line). The inset shows the same distribution in a log-log plot and the broken lines represent the two single exponential components. $n = 629$. (*D*) Experimental closed time distribution (open bars) and best fitting single exponential curve (continuous line). $n = 331$. Both distributions were obtained in hypo-osmotic conditions.

was more likely to be in the open state or in the C_1 closed state, the latter having the highest probability of occupation (53%). After stimulation by hypo-osmotic shock, the open probability increased above 50% and C_2 became the most probable closed state.

Outwardly Rectifying Channel

The fourth type of volume-sensitive chloride channel which we observed in A6 cells was characterized by an outwardly rectifying on-cell *I/V* curve (Fig. 5*A*). This channel appeared in four of the patches on basolateral membranes and in two patches on isolated cells. The average slope conductances calculated by linear regression of inward and outward currents were 15.8 ± 2.6 pS and 56.7 ± 8.1 pS respectively ($n = 6$). The open probability of the channel depended on membrane voltage. The histogram in Fig. 5*C* shows that the average values of P_o in the on-cell recordings were between 0.5 and 0.8 at negative voltages and between 0.1 and 0.5 at positive voltages when the cells were in hypo-osmotic medium. The recording in Fig. 5*D* shows the typical behavior of the channel when the voltage was alternately switched from −60 mV (phases a and c) to +60 mV (phases b and d). When holding the potential at −60 mV, the channel was almost permanently open (phases a and c). A rapid transition to +60 mV closed the channel within a few seconds (phase b and beginning of phase d); however, this voltage-induced closing did not prevent the channel from reopening without further change in voltage (end of phase d). A consequence of this behavior was that recordings of channel activity at positive holding potentials contained a larger number of opening and closing events than those at negative voltages: we therefore chose such recordings to study the evolution of the kinetic behavior of the channel when submitted to hypo-osmotic shock.

As was the case with the other channels, hypo-osmotic challenge could either stimulate an already active channel ($n = 2$) or start up a new one ($n = 4$). The delay of the response ranged between 20 sec and 3 min, with an average value of 1.5 ± 0.5 min. When the

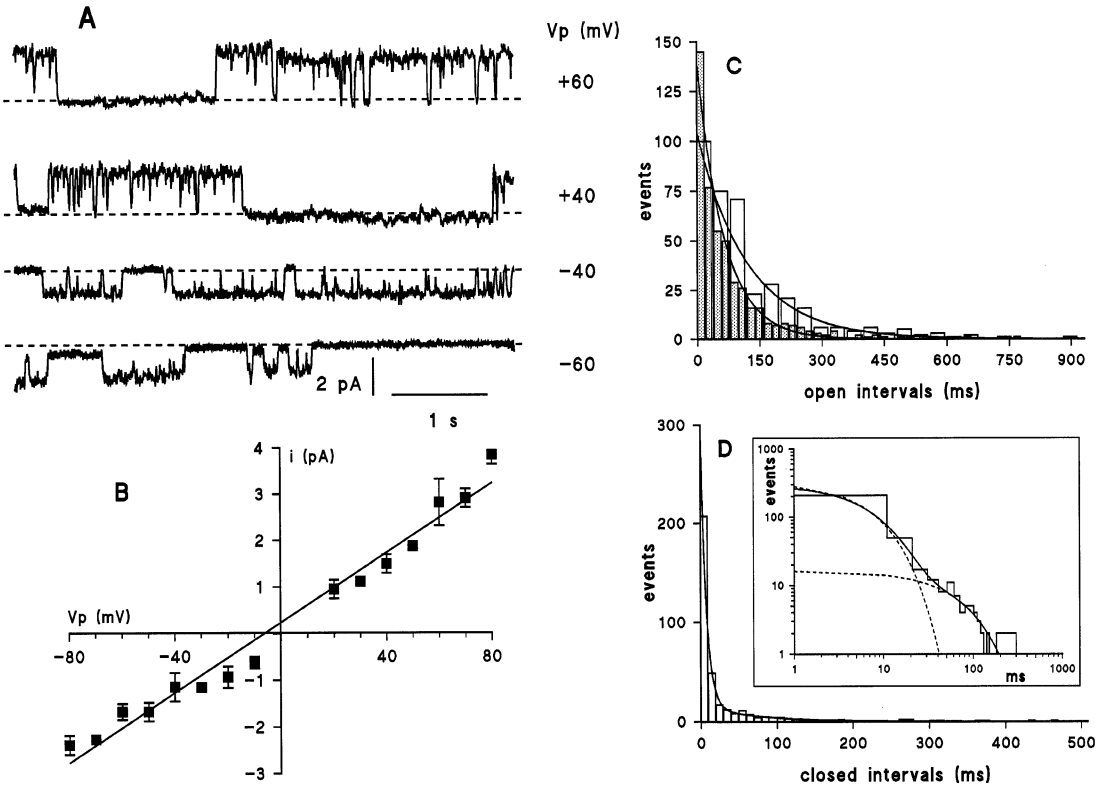

Fig. 4. Characterization of the 42 pS channel. (*A*) Recordings of the channel activity at four different holding voltages. The broken lines indicate the closed-state current levels. (*B*) Current/voltage relationship of the channel obtained by averaging the data from six independent recordings. Data were fitted by linear regression (continuous line). (*C*) Experimental open dwell-time distributions under iso-osmotic conditions (solid bars, $n = 473$) and after hypo-osmotic shock (open bars, $n = 374$). Both distributions were fitted by single exponential functions (continuous lines). (*D*) Experimental closed time distribution in hypo-osmotic conditions (open bars) and best-fitting double exponential curve (continuous line), $n = 345$. The inset shows the same distribution in a log-log plot and the broken lines represent the two single exponential components.

Table 1. Evolution of the parameters of the kinetic model for the 42 pS channel

Model: $k_{C1\to C2}\ k_{C2\to O}$ $C_1 \rightleftharpoons C_2 \rightleftharpoons O$ $k_{C2\to C1}\ k_{O\to C2}$	Iso-osmotic	Hypo-osmotic
	Rate constants (sec^{-1})	
$k_{C1\to C2}$	15.9	82.5
$k_{C2\to C1}$	96.9	13.0
$k_{C2\to O}$	81.1	11.8
$k_{O\to C2}$	18.4	7.4
	Occupation probabilities	
P_{C1}	0.53	0.07
P_{C2}	0.09	0.36
P_O	0.38	0.57

channel was already active under control conditions, hypo-osmotic stress induced an increase in the open probability from a value of 0.41 ± 0.05 to one of 0.66 ± 0.02. The distribution of open-dwell time intervals (Fig. 6*A*) was closely fitted with a single exponential function under both iso-osmotic (solid bars) and hypo-osmotic conditions (open bars). The hypo-osmotic shock increased the value of the time constant from $\tau_O = 59.1 \pm 1.2$ msec to $\tau_O = 187.3 \pm 9.1$ msec. Figure 6*B* shows the distribution of closed dwell-time intervals in a log-log plot together with the three exponential components necessary to fit the experimental data. The values of the time constants under iso-osmotic conditions were: $\tau_{C1} = 5113 \pm 235$ msec, $\tau_{C2} = 64.5 \pm 16.9$ msec and $\tau_{C3} = 17.5 \pm 1.5$ msec and became $\tau_{C1} = 1311 \pm 76$ msec, $\tau_{C2} = 90.0 \pm 8.8$ msec and $\tau_{C3} = 15.1 \pm 3.4$ msec after the shock. These data suggested that the channel had at least one open and three closed kinetic states and therefore that it could be described by a four-states kinetic model. However, since in most of the recordings a sublevel of conductance (35% of the full open conductance) was observed (indicated by the joined arrows in Fig. 6*C*), we developed a kinetic model including three closed and two open states: $C_1 \rightleftarrows C_2 \rightleftarrows C_3 \rightleftarrows O_1 \rightleftarrows O_2$ in which the O_2 state corresponded to the subconductance level. The probability of observing a subconductance event in a recording was 0.09 in control and 0.08 under hypo-

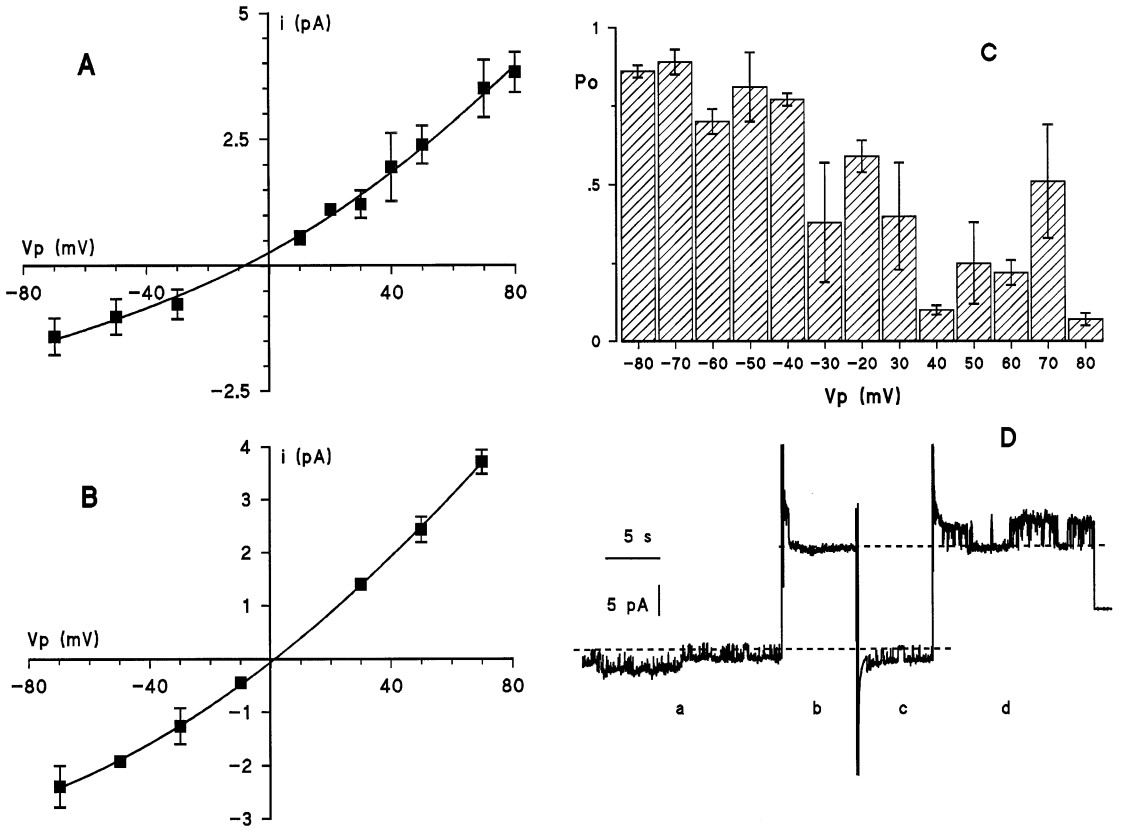

Fig. 5. Voltage dependence of the outwardly rectifying channel. (*A*) On cell *I/V* curve of the channel from the pooled recordings in basolateral membranes and on isolated cells. (*B*) Inside-out *I/V* curve recorded in presence of 151 mmol/l of chloride on both sides of the membrane. (*C*) Open probability of the channel as a function of membrane voltage. (*D*) Recording of channel activity with membrane voltage clamped alternately at −60 (phases a and c) and +60 mV (phases b and d).

osmotic conditions. Table 2 resumes the evolution of the values of the kinetic rate constants and of the occupation probabilities of the states as calculated from the model. Under both osmotic conditions, the C_1 closed state and the O_1 open state had the highest probabilities of occupation which were 0.45 and 0.35 respectively in the iso-osmotic solution. Hypo-osmotic shock decreased the probability of occupation of C_1 to a value of 0.23 and increased that of O_1 to 0.59.

We investigated the possibility that the observed outward rectification of the on-cell *I/V* curve could be entirely due to the concentration gradient of chloride ions between the pipette solution (151 mmol/l) and the intracellular medium (approximately 30 mmol/l). For this, the activity of the channel was recorded in inside-out experiments in which the choline-Cl solution was used both in the pipette and in the perfusion chamber. Under these conditions, the channel was facing symmetrical chloride ion concentrations. The *I/V* relationship of the channel recorded in these experiments still showed outward rectification, as shown in Fig. 5*B*, despite the absence of concentration gradient between the extracellular and cytoplasmic sides of the membrane. Under these conditions inward and outward conductances were 32.4 ± 2.7 pS and 57.7 ± 3.6 pS respectively.

Discussion

Comparison Between Basolateral Membranes and Isolated Cells

In general, the study of ionic channels in basolateral membranes of epithelial cells in culture suffers the major difficulty that access of the patch-clamp pipettes is hindered by the tight contact between these membranes and the support on which the cells are grown. To circumvent this difficulty, various strategies are used. Either single-channel studies are made on isolated cells [10, 17] or cultured cell monolayers are turned upside down to provide access for patch pipettes to the basolateral membranes [25, 30]. In this paper, we describe a new procedure that we have developed to detach the cell monolayer from its culture support, which was derived from that of Aceves and Erlij to isolate the frog skin epithelium from

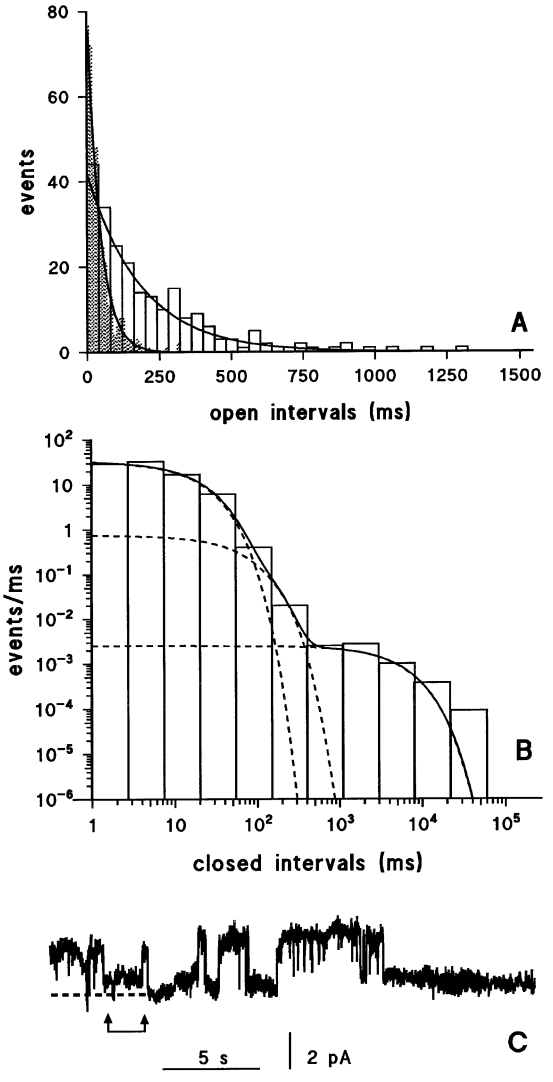

Fig. 6. Kinetic properties of the outwardly rectifying channel. (*A*) Distributions of open dwell-times in iso-osmotic conditions (solid bars, $n = 389$) and in hypo-osmotic conditions (open bars, $n = 224$) and best-fitting single exponential functions (continuous lines). (*B*) Distribution of closed dwell times in iso-osmotic conditions. Due to the large variations in the duration of closed time intervals, data were sampled with variable bin width and the number of events per time unit (events/msec) is reported in the Y axis. The continuous line represents the best-fitting triple exponential function and the broken lines represent the single exponential components. $n = 403$. (*C*) Single-channel activity of the outward rectifier when clamped at +50 mV. Joined arrows indicate the sub-conductance state of the channel. Broken line = closed level.

the chorion [1]. This allowed us to compare the results of patch-clamp experiments made on the basolateral membranes of cells in monolayers with those obtained with isolated cells. We found that the frequency of successful observations of channel activity was appreciably higher in basolateral membranes (31%) than in isolated cells (13%). Furthermore, the patches of basolateral membranes revealed a wider variety of chloride channels than was observed in isolated cells. Of the four different types of channel observed in basolateral membranes only two were seen in isolated cells. These observations indicate that organization of the cells in a monolayer is an essential condition for the functioning of some channels. The lack of spatial or functional interactions with neighboring cells must modify the intracellular organization resulting in the observed loss of activity.

Table 2. Evolution of the parameters of the kinetic model for the outwardly rectifying channel

Model: $k_{C1\to C2}\ k_{C2\to C3}\ k_{C3\to O1}\ k_{O1\to O2}$ $C_1 \rightleftharpoons C_2 \rightleftharpoons C_3 \rightleftharpoons O_1 \rightleftharpoons O_2$ $k_{C2\to C1}\ k_{C3\to C2}\ k_{O1\to C3}\ k_{O2\to O1}$		
	Iso-osmotic	Hypo-osmotic
	Rate constants (sec^{-1})	
$k_{C1\to C2}$	0.19	0.76
$k_{C2\to C1}$	1.88	2.40
$k_{C2\to C3}$	13.63	8.51
$k_{C3\to C2}$	9.64	24.50
$k_{C3\to O1}$	47.20	47.37
$k_{O1\to C3}$	10.30	3.00
$k_{O1\to O2}$	7.25	2.49
$k_{O2\to O1}$	32.38	19.00
	Occupation probabilities	
P_{C1}	0.45	0.23
P_{C2}	0.05	0.07
P_{C3}	0.07	0.03
P_{O1}	0.35	0.59
P_{O2}	0.08	0.08

Activation of Chloride Channels by Hypo-osmotic Shock

In a previous work we described how volume regulation of A6 cells after swelling in a hypo-osmotic medium is characterized by considerable increase in chloride transport rate through the basolateral membranes. Using the whole-cell patch-clamp technique we showed that the enhanced chloride transport provides a transient increase in the overall cellular chloride current as well as a transient cellular depolarization [5]. In the present single-channel study we have shown that a variety of chloride channels, whose activities were increased after hypo-osmotic shock, were present in the basolateral membranes of A6 cells. The response to osmotic stress resulted in either an activation of a quiescent channel or an increase in the activity level of a functioning one. The average delay between the beginning of the hypo-osmotic stress and the single-channel response varied between 1.5 and 3 min. This is in good agreement with the time courses of cellular depolarization and of the

increase in whole cell chloride currents, which reached their maximal values in 2 to 3 min after the shock [5]. The fact that during these single-channel recordings the osmolarity of the pipette solution was kept constant (i.e., iso-osmotic), implies that an eventual local direct control of channel activity by extracellular osmolarity would not have been detectable. Therefore, the response of the channels to volume change was most likely modulated by intracellular factors such as second messengers or modifications of the cytoskeleton.

Heterogeneity of Volume-Sensitive Channels

The activation of chloride conductances after a hypo-osmotic shock has been described at the single-channel level in several different epithelial cell types [3, 9, 28, 35]. Moreover, indirect information about the single-channel characteristics of the volume-sensitive conductance pathways has been inferred from observations of the macroscopic volume-sensitive chloride currents [2, 16, 22]. The cloning and expression of chloride channels also led to the molecular characterization of several proteins that may act as volume-sensitive channels or channel regulators: the pI_{Cln} [2, 20, 24], the ClC-2 [13], the ClC-K1 [32] and the P-glycoprotein [33].

Very often, volume-sensitive chloride channels have outwardly rectifying *I/V* curves with a slope conductance of 40 to 50 pS at reversal potential. Such channels have been found in T84 colonic cell lines [28, 35], in 407 intestinal cells in culture [22], in kidney MDCK cells [3] and in glioma C6 cells [18]. In particular, a type of outwardly rectifying channel plays a fundamental role in volume regulation owing to its permeability to a large variety of osmolytes, including anionic and zwitterionic amino acids such as glutamate and taurine [4]. This channel was first found in MDCK cells [3, 4] and was characterized in MDCK and C6 cell lines [4, 18, 19]. It was termed VSOAC for *volume sensitive organic osmolyte anion channel* [29].

Outward rectifiers, although very frequent, are not the only type of chloride channel encountered when studying the RVD process. For instance, a channel with a unitary conductance of 7 pS was found in Ehrlich ascites tumor cells [7] and evidence is given for a channel with a conductance lower than 1 pS in T84 cells [16]. Therefore, the extrusion of chloride ions and of other anionic (or neutral) osmolytes during RVD may be accomplished via different channels that sometimes coexist in one cell type, as happens in the T84 cell line.

In the present work, we have shown that four different types of volume-sensitive chloride channel are present in the basolateral membranes of A6 cells. At first, these channels were classified according to their on-cell *I/V* relationships and unitary conductances. In the on-cell recordings, three of these channels had linear *I/V* relationships, despite the gradient in chloride ion concentration between the pipette solution and intracellular medium. This implies that when exposed to symmetrical chloride concentrations they would probably show inwardly rectifying *I/V* curves. The unitary conductances of the three channels were 12, 30 and 42 pS. The kinetic behavior, as revealed by the distributions of open and closed time intervals, was different for each channel. The 12 pS channel apparently had the simplest kinetic scheme since single exponential functions could adequately fit both distributions. A double exponential function was necessary to fit the open dwell-time distribution of the 30 pS channel although a single exponential fitted the closed-time distribution. Conversely, a single exponential described the open-time distribution of the 42 pS channel but a double exponential was required for the closed-dwell times. This suggested that more complex models were necessary to describe the kinetics of these two channels. Thanks to the high degree of activity of the 42 pS channel in our recordings under both osmotic conditions, we were able to study the effect of the osmotic challenge on the behavior of this channel. The observed increase in open probability corresponded to a 2.6 times increase in the mean duration of open-time intervals. From the experimental data, we developed a kinetic model for this channel and studied the changes in the parameters of the model induced by hypo-osmotic stress. The model was characterized by two closed states and one open state ($C_1 \rightleftarrows C_2 \rightleftarrows O$). The changes in the transition rate constants provoked by channel activation resulted in an increase in P_o while the most probable closed state changed from C_1 to C_2.

The volume-sensitive chloride channel recently described by Nilius et al. [23] in isolated A6 cells has a linear on-cell *I/V* relationship with a unitary conductance of 36 pS and shows a higher open probability at depolarizing voltages than at hyperpolarizing ones. According to its unitary conductance and *I/V* relationship, this channel is comparable with both intermediate conductance channels (30 and 42 pS) which we describe in the present work. A study of its kinetic properties would probably disclose further similarities allowing better comparison with the individual types of channel. An important difference between the channel described by Nilius et al. and both the intermediate conductance channels which we found in the basolateral membranes of A6 cells, concerns the voltage dependence of the open probability. Thus, the open probabilities of the 30 and 42 pS channels are independent of voltage, as can be seen in Figs. 3*A* and 4*A* and these two channels were only recorded from basolateral membranes and never from isolated cells. The 36 pS channel on the other hand was present in isolated cells. These discrepancies are probably due to the particular cell culture conditions and to the way in which the isolated cells were obtained: they

were from subconfluent cultures in the study of Nilius et al., but were dissociated from a confluent monolayer in our work.

The fourth type of channel which we describe had an outwardly rectifying *I/V* curve when recorded in the cell-attached mode. The outward rectification of the *I/V* relationship was an intrinsic feature of this channel and did not depend exclusively on the chloride ion concentration gradient between the pipette solution and the cytoplasm. In fact, the rectification was still present, although less pronounced, in the inside-out recordings, where identical solutions were used on both sides of the membrane. The model we developed to describe the kinetic characteristics of this channel had three closed and two open states ($C_1 \rightleftarrows C_2 \rightleftarrows C_3 \rightleftarrows O_1 \rightleftarrows O_2$). Unlike the 42 pS channel, the outward rectifier did not significantly modify the pattern of occupation probabilities of the states upon stimulation in the hypo-osmotic medium. The most probable states were C_1 and O_1 in both experimental conditions. A purely speculative interpretation of this difference would be the existence of two different mechanisms underlying the activation of these channels.

The presence of four different types of chloride channel in the basolateral membrane of A6 cells may reveal the important role played by this ion in cellular homeostasis. The fact that some of the channels described in this paper were already active in unswollen cells would indicate that they may participate in housekeeping process or in transepithelial chloride transport, occurring in parallel with sodium reabsorption in resting cells [8]. Our results also show that the 12 pS channel was the most frequently evoked during the regulatory volume decrease after a serosal hypo-osmotic shock. The other channels might eventually be more involved in volume regulation after swelling caused by unbalanced transport rates across the opposite membranes. Furthermore, some channels could also be involved in transport of osmolytes other than chloride, as it will be discussed in the next paragraphs.

The outwardly rectifying channel showed some important similarities with other volume-sensitive chloride channels. Figure 5*C* shows the open probability of this channel as a function of membrane potential in hypo-osmotic conditions. At hyperpolarizing voltages P_o was close to unity and decreased below 0.5 at depolarizing voltages. Similar responses were also observed for the outwardly rectifying channel found in MDCK cells and in C6 cells: the VSOAC [3, 18]. Jackson and Strange [18] showed that activation of the VSOAC in C6 cells held at a negative cellular potential, occurs by an abrupt switching of the open probability from zero to a value close to unity. This channel, once stimulated, inactivates within a few seconds after membrane depolarization. The decrease in P_o observed in the outwardly rectifying channel in A6 cells at depolarizing voltages was also related to a fast closure of the channel induced by depolarization (Fig. 5*D*). However, in this case, the channel did not inactivate completely, since spontaneous reopenings at the same holding potential were possible. From a kinetic point of view, the model that best described the behavior of the A6 outward rectifier included three closed states. A similar kinetic model including three inactive states was proposed by Jackson and Strange to describe the inactivation process of the VSOAC of C6 cells as a function of voltage [19].

These similarities are obviously not sufficient to conclude that the outwardly rectifying channel of A6 cells actually is a VSOAC. They simply point to some common features of volume-sensitive anion channels and only studies on the selectivity properties of the channel will provide the answer to the question. The individual characterization of the four types of channel described in this work will also be enhanced by the identification of the intracellular mechanisms underlying their activation in hypo-osmotic conditions and by the study of the blocking effects of drugs specific to chloride channels.

References

1. Aceves, J., Erlij, D. 1971. Sodium transport across the isolated epithelium of the frog skin. *J. Physiol.* **212:**195–210
2. Ackerman, M.J., Wickman, K.D., Clapham, D.E. 1994. Hypotonicity activates a native chloride current in *Xenopus* oocytes. *J. Gen. Physiol.* **103:**153–179
3. Banderali, U., Roy, G. 1992*a*. Activation of K^+ and Cl^- channels in MDCK cells during volume regulation in hypotonic media. *J. Membrane Biol.* **126:**219–234
4. Banderali, U., Roy, G. 1992*b*. Anion channels for amino acids in MDCK cells. *Am. J. Physiol.* **263:**C1200–C1207
5. Brochiero, E., Banderali, U., Lindenthal, S., Raschi, C., Ehrenfeld, J. 1995. Basolateral membrane chloride permeability of A6 cells: implication in cell volume regulation. *Pfluegers Arch.* **431:**32–45
6. Broillet, M.C., Horisberger, J.D. 1991. Basolateral membrane potassium conductance of A6 cells. *J. Membrane Biol.* **124:**1–12
7. Christensen, O., Hoffmann, E.K. 1991. Cell swelling activates K^+ and Cl^- channels as well as nonselective, stretch-activated cation channels in Ehrlich ascites tumor cells. *J. Membrane Biol.* **129:**13–36
8. Crowe, W.E., Ehrenfeld, J., Brochiero, E., Wills, N.K. 1995. Apical membrane sodium and chloride entry during osmotic swelling of renal (A6) epithelial cells. *J. Membrane Biol.* **144:**81–91
9. Diener, M., Nobles, M., Rummel, W. 1992. Activation of basolateral Cl^- channels in the rat colonic epithelium during regulatory volume decrease. *Pfluegers Arch.* **421:**530–538
10. Dietl, P., Stanton, B.A. 1992. Chloride channels in apical and basolateral membranes of CCD cells (RCCT-28A) in culture. *Am. J. Physiol.* **273:**F243–F250
11. Ehrenfeld, J., Raschi, C., Brochiero, E. 1994. Basolateral potassium membrane permeability of A6 cells and cell volume regulation. *J. Membrane Biol.* **138:**181–195
12. Granitzer, M., Bakos, P., Nagel, W., Crabbe, J. 1991. Osmotic swelling and membrane conductances in A6 cells. *Biochim. Biophys. Acta.* **1110:**239–242
13. Gründer, S., Thiemann, A., Pusch, M., Jentsch, T.A. 1992. Regions

involved in the opening of ClC-2 chloride channel by voltage and cell volume. *Nature*. **360:**759–762

14. Hamill, O.P., Marty, A., Neher, E., Sakmann, B., Sigworth, F.J. 1981. Improved patch-clamp techniques for high resolution current recording from cells and cell-free membrane patches. *Pfluegers Arch.* **391:**85–100
15. Handler, J.S., Steele, R.E., Sahib, M.K., Wade, J.B., Preston, A.S., Lawson, N.S.L., Johnson, J.P. 1979. Toad urinary bladder epithelial cells in culture: maintenance of epithelial structure, sodium transport, and response to hormones. *Proc. Natl. Acad. Sci. USA* **76:**4151–4155
16. Ho, M.W.Y., Duszyk, M., French, A.S. 1994. Evidence that channels below 1 pS cause the volume sensitive chloride conductance in T84 cells. *Biochim. Biophys. Acta* **1191:**151–156
17. Hunter, M. 1990. Stretch activated channels in the basolateral membrane of single proximal cells of frog kidney. *Pfluegers Arch.* **416:**448–453
18. Jackson, P.S., Strange, K. 1995*a*. Single-channel properties of a volume-sensitive anion conductance. *J. Gen. Physiol.* **105:**643–660
19. Jackson, P.S., Strange, K. 1995*b*. Characterization of the voltage-dependent properties of a volume-sensitive anion conductance. *J. Gen. Physiol.* **105:**661–677
20. Krapivinsky, G.B., Ackerman, M.J., Gordon, E.A., Krapivinsky, L.D., Clapham, D.E. 1994. Molecular characterization of a swelling-induced chloride conductance regulatory protein pI_{Cln}. *Cell* **76:**439–448
21. Krouse, M.E., Haws, C.M., Xia, Y., Fang, R.H., Wine, J.J. 1994. Dissociation of depolarization-activated and swelling-activated Cl^- channels. *Am. J. Physiol.* **267:**C642–C649
22. Kubo, M., Okada, Y. 1992. Volume-regulatory Cl^- channel currents in cultured human epithelial cells. *J. Physiol.* **456:**351–371
23. Nilius, B., Sehrer, J., De Smet, P., Van Driessche, W., Droogmans, G. 1995. Volume regulation in a toad epithelial cell line: role of coactivation of K^+ and Cl^- channels. *J. Physiol.* **487.2:**367–378
24. Paulmichl, M., Li, Y., Wickman, K., Ackerman, M., Peralta, E., Clapham, D. 1992. New mammalian chloride channel identified by expression cloning. *Nature* **356:**238–241
25. Ponce, A., Cereijido, M. 1991. Polarized distribution of cation channels in epithelial cells. *Cell Physiol. Biochem.* **1:**13–23
26. Reuss, L., Cotton, C.U. 1994. Volume regulation in epithelia: Transcellular transport and cross-talk. *In:* Cellular and molecular physiology of cell volume regulation. K. Strange, Editor. pp. 31–47. CRC Press
27. Sigworth, F.J., Sine, S.M. 1987. Data transformation for improved display and fitting of single channel dwell time histograms. *Biophys. J.* **52:**1047–1054
28. Solc, C.K., Wine, J.J. 1991. Swelling-induced and depolarization-induced Cl^- channels in normal and cystic fibrosis epithelial cells. *Am. J. Physiol.* **261:**C658–C674
29. Strange, K., Jackson, P.S. 1995. Swelling-activated organic osmolyte efflux: A new role for anion channels. *Kidney Int.* **48:**994–1003
30. Tabcharani, J.A., Harris, R.A., Boucher, A., Eng, J.W.L., Hanrahan, J.W. 1991. Basolateral K channels activated by carbachol in the epithelial cell line T_{84}. *J. Membrane Biol.* **142:**241–254
31. Ubl, J., Murer, H., Kolb, H.A. 1988. Ion channels activated by osmotic and mechanical stress in membranes of opossum kidney cells. *J. Membrane Biol.* **104:**223–232
32. Uchida, S., Sasaki, S., Furukawa, T., Hirakota, M., Imai, T., Hirata, Y., Marumo, F. 1993. Molecular cloning of a chloride channel that is regulated by dehydration and expressed predominantly in kidney medulla. *J. Biol. Chem.* **268:**3821–3824
33. Valverde, M.A., Diaz, M., Sepúlveda, F.V., Gill, D.R., Hyde, S.C., Higgins, C.F. 1992. Volume-regulated chloride channels associated with the human multidrug-resistance P-glycoprotein. *Nature* **355:**830–833
34. Verrey, F., Schaerer, E., Zoerkler, P., Paccolat, M.P., Geering, K., Kraehenbuhl, J.P., Rossier, B.C. 1987. Regulation by aldosterone of Na^+,K^+-ATPase mRNAm, protein synthesis, and sodium transport in cultured kidney cells. *J. Cell Biol.* **104:**1231–1237
35. Worrell, R.T., Butt, A.G., Cliff, W.H., Frizzell, R.A. 1989. A volume sensitive chloride conductance in human colonic cell line T_{84}. *Am. J. Physiol.* **256:**C1111–C1119